Eur. Phys. J. D **7**, 229–234 (1999)

THE EUROPEAN PHYSICAL JOURNAL D

EDP Sciences

Species selective evaporation during surface scattering of binary van der Waals clusters

E. Fort[a], H. Vach, A. De Martino, M. Châtelet, and F. Pradère

Laboratoire d'Optique Quantique du CNRS, Ecole Polytechnique, 91128 Palaiseau Cedex, France

Received: 28 January 1999

Abstract. We performed both experiments and molecular dynamics simulations for the scattering of mixed $Ar_{880}Kr_{120}$ from a graphite surface under conditions where evaporation of thermalized small fragments is the main channel to evacuate the excess collision energy of the cluster impact. In spite of the expected thermal nature of the scattering process, we find average temperatures for the evaporating cluster particles that are considerably higher for krypton than for argon. We discuss the possible influence of the involved binding energies and the probable role of the incident cluster structure on these new results.

PACS. 36.40.-c Atomic and molecular clusters – 34.30.+h Intramolecular energy transfer; intramolecular dynamics; dynamics of van der Waals molecules – 68.10.Jy Kinetics (evaporation, adsorption, condensation, catalysis, etc.)

1 Introduction

The interaction dynamics between pure van der Waals (vdW) clusters and surfaces has been studied extensively in the last few years. More recently, surface scattering involving binary vdW clusters has gained much interest, partly motivated by the potential of cluster impact induced chemical reactions [1–4].

Pure or mixed vdW clusters have the same kind of dynamics when colliding with a surface at low incident kinetic energies [5–19]. For these low energies, the dominant mechanism is evaporative; *i.e.*, the impinging clusters undergo a kind of Leidenfrost phenomena: they slide along the surface on a gaseous "cushion" of cluster atoms that limits the energy exchange with the surface. As they slide, the clusters evaporate thermalized small fragments (mainly monomers) to dissipate the normal kinetic energy of the impact, while the tangential velocity is mainly conserved. If the energy of the collision is not sufficiently high to evaporate the entire cluster, a relatively large surviving cluster fragment is expected to be scattered in a grazing angle direction [17].

Investigating mixed vdW cluster collision dynamics in an earlier work, we have shown that the surface scattering process is species selective by measuring the composition change between the surviving cluster and the impinging one [5,6]. Studying the enrichment of the surviving fragment in the dopant species for mixed incident clusters obtained by pick-up of krypton or xenon on neat argon clusters, we have shown that the evaporation process cannot be considered as a simple distillation. We pointed out the crucial role played by the details of the incident cluster structure to interpret the results. This interpretation has been confirmed by molecular dynamics (MD) simulations on the structure of large mixed clusters undergoing a realistic pick-up [20].

In this paper, we focus our attention on the evaporation process, which is the main scattering channel at low incident kinetic energies. Using mixed vdW clusters, we show that the evaporation temperature is species dependent. This result gives new insights in the possible use of the cluster dopant species as a probe of the collision dynamics. Moreover, we discuss how it can open new ways to investigate the cluster structures.

This paper is structured as follows: the experimental setup is described in section 2 together with our data analysis scheme, section 3 is devoted to the technical details of the MD simulations. Our results are presented and discussed in section 4.

2 Experimental setup and data analysis

Our experimental setup has been described in detail previously [21]. In this section, we only summarize the essential parts that are of interest for the new results presented in the following. We use a supersonic Campargue-type beam generator with a conical nozzle (with a 0.12 mm diameter and 5° half-angle). The beam passes through three differentially pumped chambers before entering an Ultra-High Vacuum (UHV) chamber. We can introduce a buffer gas in the third chamber either directly to permit average cluster size determination [22] or through a small pipe in the beam path for the pick-up process [6].

[a] e-mail: fort@leonardo.polytechnique.fr

Beam diagnostics are performed using a rotatable Quadrupole Mass Spectrometer (QMS) in the UHV chamber. The QMS mass range extends to 200 amu and can consequently only detect relatively small particles. When larger fragments enter the ionization head of the QMS, they are fragmented into small particles before being detected. The QMS rotates about the center of the UHV chamber where a surface sample can be placed to intercept the beam. The beam is modulated by a chopper placed in the third vacuum chamber to allow flux lock-in detection and time-of-flight (TOF) measurements. Our experimental configuration allows us to retrieve the velocity distribution of the particles before and after the surface collision.

The mixed clusters are obtained in the third chamber by pick-up of krypton on pure argon clusters. The neat argon cluster velocity is about (560 ± 20) m/s and is reduced to (470 ± 20) m/s due to the krypton pick-up. To compare the results obtained for mixed clusters with those for pure clusters, we use argon as buffer gas to slow the pure argon clusters down to the same velocity as the doped krypton ones.

The relative composition of the mixed clusters is obtained from QMS flux measurements directly within the cluster beam at each species mass setting after sensitivity corrections. The krypton molar fraction is given within 10% uncertainty. The QMS has been calibrated for the involved species with a Bayard-Alpert gauge in the UHV chamber by introducing a pressure-controlled residual gas through a microvalve.

The size of the clusters is determined by the profile broadening technique [22]. When passing through a buffer gas, the beam profile broadens. From the measurement of this broadening as a function of the buffer gas pressure, it is possible to deduce the average cluster size. Our experimental setup does not allow us to measure the cluster size when employing the pick-up technique. Nevertheless, simple energetic considerations [5] prove that the pick-up process does not significantly change the cluster size for large clusters as those considered in the present paper. The size of the mixed clusters remains in the uncertainty of the size measurement technique, which is of about 50%.

In the present paper, the surface used is a Highly Oriented Pyrolytic Graphite (HOPG) sample at a temperature of 550 K and an incidence angle of 30°. The average mixed and pure argon clusters are $Ar_{880}Kr_{120}$ and Ar_{1000}, respectively. Their velocity when colliding with the surface is (470 ± 20) m/s.

As mentioned in the introduction, for low incident kinetic energies the dynamics of the vdW cluster collision with a surface can be understood as follows: the cluster impinging with a certain incidence angle slides on the surface on a gaseous cushion while evaporating thermalized small particles.

Apart from this main evaporation channel, two other scattering channels can be detected: the diffusion channel composed of cluster particles that undergo a trapping/desorption process and a grazing channel of slow and large fragments that survive the collision.

Due to surface scattering, particles evaporate from the parent cluster mainly as a result of the normal kinetic energy redistribution into the cluster's internal degrees of freedom. It is possible to define an average local temperature $T_{\rm loc}$ from the experimental data. We have developed a model [11] in which cluster particles are evaporated at this temperature $T_{\rm loc}$ from a cluster frame moving with a velocity of $c_{\rm f} v_{\parallel}$, where $c_{\rm f}$ is the conservation coefficient of the incident velocity component parallel to the surface $v_{\parallel}$. This model fits very well the experimental results in the evaporation regime for a large range of experimental conditions for the surface scattering of both mixed and pure clusters. The normalized scattered particle flux profiles are fitted with the only parameter $c_{\rm f}$. This latter is then used to fit the TOF profiles to retrieve the local temperature $T_{\rm loc}$.

3 Molecular dynamics simulations

To compare our experimental results with those from simulations, we have performed MD calculations of the surface scattering of mixed cluster. In the following, we describe the intracluster atomic interactions by pairwise 6-12 Lennard-Jones potentials [23] that are truncated at a cutoff distance $r_{\rm cut}$ of 2.5σ [24]:

$$u(r_{ij}) = 4\epsilon_{ij}\left[\left(\frac{\sigma_{ij}}{r_{ij}}\right)^{12} - \left(\frac{\sigma_{ij}}{r_{ij}}\right)^{6}\right], \qquad (3.1)$$

where r_{ij} is the distance between particles i and j, and ϵ_{ij} and σ_{ij} are the usual Lennard-Jones parameters for interatomic potential well depth and distance, respectively. We use the same Lennard-Jones σ_{ij} and ϵ_{ij} values as those employed by Perera and Amar for their simulation of the pick-up process [25].

The equations of motion are integrated using Gear's fifth-order predictor-corrector algorithm [24,26,27] with a time step Δt of 10 fs which assures good conservation of energy throughout the whole simulation: the relative energy conservation error is usually smaller than 10^{-9}. Repeating several of our calculations with a time step of only 1 fs, we found all results unchanged within their statistical uncertainties. We also recalculated several selected trajectories without any cutoff radius, but did not find any significant deviation from the results with $r_{\rm cut} = 2.5\sigma$.

To assure a realistic structure of the incident mixed clusters, we have simulated the pick-up process under conditions very similar to those of our experiment [20]. The most important result of this study for the present work can be summarized as follows: we performed the pick-up procedure for five Ar_{904} at 32 K [28] with randomly chosen initial orientation and incident velocities between 575 and 625 m/s which assured a sufficiently good signal-to-noise ratio. The pick-up under the experimental conditions considered here led to an average cluster composition of $Ar_{880}Kr_{120}$. After about 1 μs of free flight after the buffer gas cell, those mixed clusters had a temperature of (32 ± 5) K and a velocity of (470 ± 30) m/s. The guest

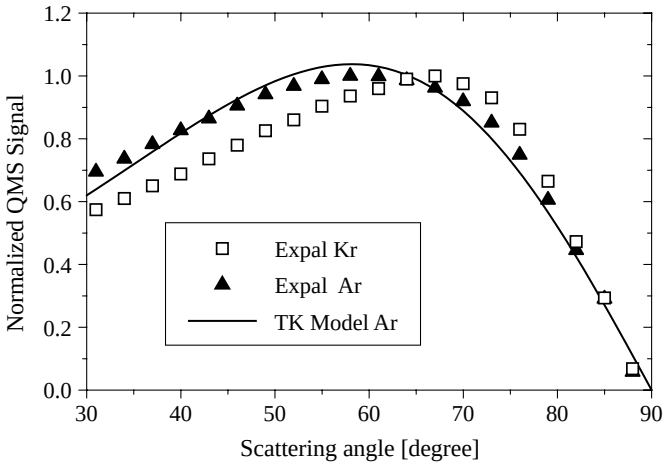

Fig. 1. Normalized flux distributions *versus* scattering angle for mixed $Ar_{880}Kr_{120}$ clusters colliding on a HOPG surface at 550 K with an incident velocity of 470 m/s and incidence angle of 30°. Triangles: argon; open squares: krypton; full line: fit obtained using the thermokinetic (TK) model for argon.

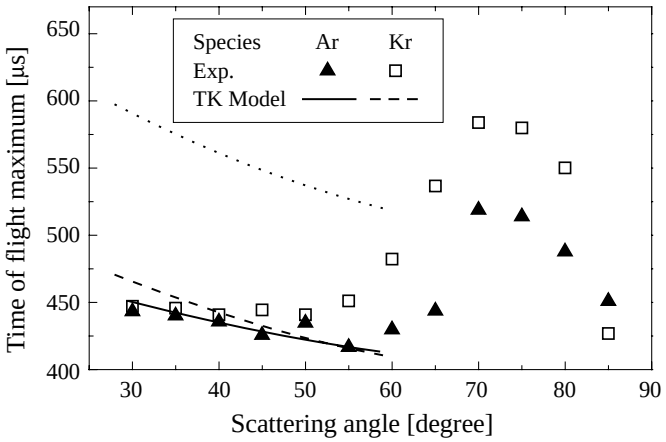

Fig. 2. Temporal position of the maxima of the experimental TOF profiles distribution *versus* scattering angle for krypton (open squares) and argon (triangles) for mixed $Ar_{880}Kr_{120}$ clusters colliding on a HOPG surface at 550 K with an incident velocity of 470 m/s and incidence angle of 30°. Fits obtained from the thermokinetic (TK) model: dashed line for krypton and full line for argon. The dotted line indicates the krypton TOF maximum profile if the two species would have been in thermal equilibrium.

krypton atoms were always found to be homogeneously distributed within the two or three outermost atomic layers of the mixed cluster, which is in good qualitative agreement with the findings of Perera and Amar [25].

In the present work, we simulate the binary cluster scattering from a perfectly hard surface without any energy exchange between the surface and the scattering cluster. To this end, we place the surface in the x-y plane of our coordinate system and assume perfectly hard collisions for each cluster atom that touches the surface; *i.e.*, whenever a cluster atom arrives on the surface, we simply reverse its z velocity component while we leave its x and y velocity components unchanged. As a result, surface scattered cluster atoms impact into the approaching parent cluster leading to heating of the binary cluster and consequently to the evaporation of small cluster fragments (mainly monomers): the smaller the incident angle, the higher the evaporation rate and the smaller the outcoming surviving cluster. Every ten time steps, we calculate the instantaneous cluster temperature $T_{\rm vib}$ and the kinetic energies $E_{\rm kin}$ of the evaporated cluster atoms in the moving frame of the scattering cluster. The latter allows us then, in a very straightforward manner, to determine an instantaneous temperature $2E_{\rm kin}/3k_{\rm B}$, where $k_{\rm B}$ is the Boltzmann constant. Averaging this temperature over the whole evaporation process leads then directly to a temperature that corresponds to the experimentally determined local temperature $T_{\rm loc}$.

4 Results and discussion

Figure 1 shows the experimentally determined normalized flux distributions of the scattered argon and krypton particles for mixed $Ar_{880}Kr_{120}$ clusters impinging on a graphite surface with a velocity of 470 m/s and an incidence angle of 30°. The two lobes are very much the same for both species: they are smooth and centered at 60° and 70° for argon and krypton, respectively. The krypton profile is slightly narrower and more grazing than the argon one. Both distributions are fitted using the thermokinetic (TK) model to retrieve the conservation coefficient of the tangential velocity $c_{\rm f}$. The fit obtained from the argon distribution is presented in Figure 1. The fits give a $c_{\rm f}$ value of 0.9 ± 0.05 for both species as expected since the moving frame is the same. The good conservation of the tangential velocity is directly related to the flatness of the employed HOPG surface. Besides, the fits by the TK model yield a ratio of krypton and argon fluxes scattered in 2π sr equal to 0.2 ± 0.04. This value is in reasonable agreement with the incident cluster composition. The difference can be attributed to the in-plane limited measurements and the existence of other scattering channels.

Figure 2 shows the temporal position of the maxima of the experimental TOF profiles *versus* scattering angle for krypton and argon for the same experimental conditions as in Figure 1. The two curves are very much alike for both species. From 30 to 55°, the scattered particles are faster than for grazing angles and their velocity slightly increases with increasing scattering angle. On the contrary, for scattering angles larger than 60°, the particle velocity decreases sharply. This velocity dependence on the scattering angle is very characteristic of the evaporation regime [11]. Between 30 and 55°, the evaporation channel is dominant. The increase of the velocity with scattering angle is readily explained by the fact that the particles are scattered from a moving frame. In the grazing direction, the surviving clusters are detected in addition to small evaporating fragments. The relative importance of the surviving clusters increases with increasing scattering angle. The velocity of these large fragments is rather slow

Table 1. Local temperatures resulting from mixed $Ar_{880}Kr_{120}$ and pure Ar_{1000} clusters colliding on a graphite surface with an incident velocity of 470 m/s and incidence angle of 30°.

Cluster type		$Ar_{880}Kr_{120}$	Ar_{1000}
Experimental	T_{loc}(Ar) [K]	190 ± 30	180 ± 30
	T_{loc}(Kr) [K]	280 ± 30	
MD simulations	T_{loc}(Ar) [K]	110 ± 10	102 ± 5
	T_{loc}(Kr) [K]	190 ± 20	

since the surviving clusters have only a negligible normal velocity and only 90% of the incident tangential velocity, *i.e.* $c_f v_{\|}$.

As a consequence, the fit using the TK model must be limited to the range of scattering angles between 30 and 55°, for which the main channel for the scattered particles is the evaporation one. For smaller and especially for negative scattering angles, the diffusion channel, due to particles undergoing a trapping/desorption mechanism [12], is not negligible any more compared with the evaporation channel. The TK model fits are also presented in Figure 2 for argon and krypton, using the $c_f = 0.9$ value obtained from the flux distributions. In addition, Figure 2 (see dotted line) shows the result of the TK model if krypton particles were scattered with the same temperature as argon atoms. Clearly, simple thermal equilibration between argon and krypton would have resulted in much slower velocities for krypton than the ones we measured experimentally.

Table 1 presents the temperature T_{loc} obtained with the TK model from the experimental data for both mixed $Ar_{880}Kr_{120}$ and pure Ar_{1000} clusters impinging under the same conditions. It also shows the results obtained with our MD simulations. The experimental evaporation temperature is about 90 K higher for krypton (T_{loc}(Kr) = 280 ± 30 K) than for argon (T_{loc}(Ar) = 190 ± 30 K). From our MD simulations, we obtain about the same difference 80 K between the two species local temperatures: $T_{loc}(Kr) = 190 \pm 20$ K and $T_{loc}(Ar) = 110 \pm 10$ K. In addition, we find that the scattering clusters reach their maximum instantaneous vibrational temperatures of about 210 K after only 10 ps just before the thermal particle evaporation becomes significant. The center-of-mass motion in the z-direction is reversed after about 18 ps which coincides with the minimum in cluster density: at this point the density is reduced by about one order of magnitude. The presently neglected net energy transfer from the graphite surface to the scattering cluster is most probably responsible for the lower local temperatures obtained from MD simulations as compared to the experimental ones.

In Figure 3, we display three snapshots of the collision. Figure 3a shows a typical mixed cluster of $Ar_{880}Kr_{120}$ produced by a realistic pick-up before it collides onto the surface. Figure 3b shows how an incident cluster flattens out on the surface due to its impact validating one of our major assumptions in the derivation of the TK model [11]. A typical surviving large cluster fragment of $Ar_{380}Kr_{59}$ is presented in Figure 3c. Experimental evidence of this kind of fragments scattered at grazing angles is given by the positive slope of the TOF distribution *versus* scattering angle presented in Figure 2. As in the experiment, the surviving cluster has undergone a krypton enrichment during the collision process [5].

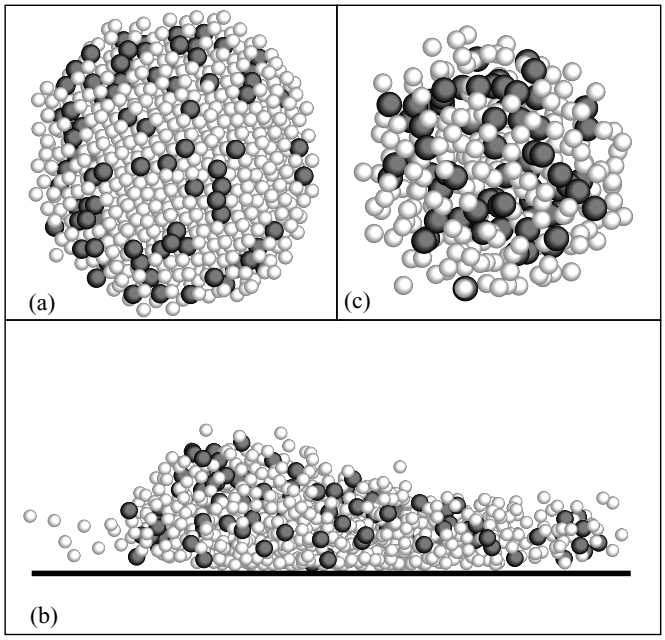

Fig. 3. Three snapshots of a typical $Ar_{880}Kr_{120}$ cluster scattering off a hard surface: a) initial cluster structure after realistic pick-up, b) snapshot at 10 ps after surface impact and c) snapshot of the surviving binary cluster 50 ns after its surface interaction.

The large difference in local temperature for the two species thermally evaporating from the same cluster is certainly the most intriguing result. We first address the question if the difference in binding energy for the two species could possibly explain the temperature difference. The binding energy of krypton is larger than that of argon (173 K *versus* 120 K). Nevertheless, for a given constant cluster temperature, this difference is not expected to have any influence on the local temperature: both species should evaporate in equilibrium with the instantaneous vibrational temperature of the parent cluster [5]. The instantaneous vibrational temperature of the cluster, however, is not constant during the collision process. It evolves, in general, as the result of energy transfers from the incident kinetic energy, from the exchange with the surface and toward the evaporation process [29]. The measured TOF profiles for the evaporating fragments can, consequently, be considered as a superposition of many Boltzmannian profiles at different instantaneous cluster temperatures. In addition, the relative rates of evaporation depend on both binding energy and instantaneous temperature. Therefore, the average local temperature T_{loc} that we measure [11] does depend on the species binding energy.

Our MD simulations of the collision show that the cluster reaches a maximum vibrational temperature of 210 K. Performing simple calculations with Arrhenius evaporating rates applied to the vibrational temperature profile, we found that the resulting temperature difference cannot account for more than a few degrees between the two-species local temperatures. Indeed, the proportion of particles evaporating while the cluster vibrational temperature is maximal is relatively low. The cluster reaches its vibrational temperature maximum very rapidly (within about 10 ps) before evaporation becomes significant due to the very high heating rates during the surface collision. Then, the cluster temperature rapidly decreases by ejection of non-thermal particles. Nevertheless, the "thermal evaporation" interpretation of the collision dynamics remains valid, since only very few atoms are involved during this rapid non-thermal cooling for our experimental conditions. The large majority of scattered particles evaporate during the following few pico-seconds in thermal equilibrium with the instantaneous vibrational temperature of the parent cluster. Collisions between atoms after evaporation are very unprobable as shown in our MD simulations. These results are in excellent agreement with the findings of Svanberg *et al.* [29] for pure large argon cluster scattering from Pt(111) surface with low collision velocities.

For higher incident velocities, a shattering regime is expected to open up for which a shock wave propagates into the incident cluster and the scattered particles are not thermalized any more, but directly ejected. MD simulation on mixed Ne_nAr_m clusters have shown that the ejection velocity is, indeed, species dependent [16]. We want to underline, however, that the experimental conditions considered in the present paper are not in the same energy regime; for instance, we did not detect any fast particles at grazing angles. Therefore, we have to reject the possibility of an activated process to explain the considerable difference in local temperatures for the two species.

In a previous paper, we have shown that the evaporation process could not be considered as a simple distillation to explain the results on the composition change between incident and surviving clusters [5]. We pointed out the crucial role played by the details of the incident cluster structure and confirmed our conclusions by a comprehensive MD simulation study of the pick-up process [20]. Our present calculations show that the incident cluster does not undergo a complete reorganization during the collision and that the dynamics of the collision is, consequently, strongly influenced by the incident cluster structure: note for instance in Figure 3b, which has been recorded 10 ps after the impact, that the majority of the krypton atoms are still very close to the cluster surface giving them a higher probability to leave the cluster at the beginning of the evaporation process than if they were inside the cluster. Consequently, krypton is expected to evaporate prior to the main part of argon atoms. We can, therefore, consider that krypton probes the vibrational temperature of the parent cluster at an earlier time in the scattering process than argon. Finally, we like to mention that the evaporation dynamics of argon seems to be little affected by the presence of the low krypton concentration giving similar local temperatures for pure Ar_{1000} and mixed $Ar_{880}Kr_{120}$ clusters. The slightly higher argon scattering temperature for the mixed cluster might simply be due to the increase in the incident kinetic energy per atom (about 10%) for the mixed clusters since krypton is heavier than argon.

5 Conclusion

Based on both experiments and MD simulations, we argue that the average temperature of small fragments evaporating from mixed $Ar_{880}Kr_{120}$ clusters colliding with a graphite surface for low kinetic energy is species dependent. The average krypton temperature is about 280 K while the argon one is only 190 K. This difference agrees with the relative binding energies of the two species. Considering, however, the vibrational temperature profile of the parent cluster during the collision, the difference in binding energies can only account for a temperature difference of a few degrees, but not for 90 K. We propose, consequently, that the initial cluster structure plays a crucial role for the details of the scattering mechanism. Our MD simulations show that krypton remains near the cluster surface during the entire surface interaction. Therefore, the krypton atoms can readily evaporate at the very onset of the significant particle evaporation occurring just after the cluster obtained its maximum vibrational temperature. The importance of incident cluster structure in the collision dynamics is confirmed by our previous results on the composition of the surviving clusters [5]. Hence, the different dopant species could be considered as a probe for the collision dynamics and, hence, the scattering dynamics could possibly be used as a new means to investigate the mixed cluster structure.

References

1. J.N. Beauregard, H.R. Mayne, J. Chem. Phys. **99**, 6667 (1993).
2. S.A. Klopcic, M.F. Jarrold, J. Chem. Phys. **106**, 8855 (1997).
3. T. Raz, R.D. Levine, Chem. Phys. Lett. **246**, 405 (1995).
4. M. Gupta, E.A. Walters, N.C. Blais, J. Chem. Phys. **104**, 100 (1996).
5. E. Fort, A. De Martino, F. Pradère, M. Châtelet, H. Vach, J. Chem. Phys. **110**, 2579 (1999).
6. F. Pradère, M. Benslimane, M. Châtelet, A. De Martino, H. Vach, Surf. Sci. Lett. **375**, L375 (1997).
7. E.W. Becker, R. Klingelhofer, H. Mayer, Z. Naturforsch. A **23**, 274 (1968).
8. J. Gspann, G. Krieg, J. Chem. Phys. **61**, 4037 (1974).
9. R.J. Holland, G.Q. Xu, J. Levkoff, A. Robertson Jr., S.L. Bernasek, J. Chem. Phys. **88**, 7952 (1988).
10. M. Châtelet, A. De Martino, J. Pettersson, F. Pradère, H. Vach, Chem. Phys. Lett. **196**, 563 (1992).
11. H. Vach, A. De Martino, M. Benslimane, M. Châtelet, F. Pradère, J. Chem. Phys. **100**, 3526 (1994).

12. M. Benslimane, M. Châtelet, A. De Martino, F. Pradère, H. Vach, Chem. Phys. Lett. **237**, 223 (1995).
13. C. Menzel, A. Knoner, J. Kutzner, H. Zacharias, Z. Phys. D **38**, 179 (1996).
14. G.Q. Xu, S.L. Bernasek, J.C. Tully, J. Chem. Phys. **88**, 3376 (1988).
15. J.B.C. Pettersson, N. Marković, Chem. Phys. Lett. **201**, 421 (1993).
16. N. Marković, J.B.C. Pettersson, J. Chem. Phys. **100**, 3911 (1994).
17. H. Vach, M. Benslimane, M. Châtelet, A. De Martino, F. Pradère, J. Chem. Phys. **103**, 1972 (1995).
18. M. Svanberg, N. Marković, J.B.C. Pettersson, Chem. Phys. **201**, 473 (1995).
19. M. Svanberg, J.B.C. Pettersson, Chem. Phys. Lett. **263**, 661 (1996).
20. H. Vach, Phys. Rev. B **59**, 13413 (1999).
21. F. Pradère, M. Benslimane, M. Chateau, M. Bierry, M. Châtelet, D. Clement, A. Guilbaud, J.-C. Jeannot, A. De Martino, H. Vach, Rev. Sci. Instrum. **65**, 161 (1994).
22. A. De Martino, M. Benslimane, M. Châtelet, C. Crozes, F. Pradère, H. Vach, Z. Phys. D **27**, 185 (1993).
23. G.C. Maitland, M. Rigby, E.B. Smith, W.A. Wakeham, *Intermolecular Forces* (Clarendon Press, Oxford, 1981).
24. M.P. Allen, D.J. Tildesley, *Computer Simulations of Liquids* (Clarendon Press, Oxford, 1987).
25. L. Perera, G. Amar, J. Chem. Phys. **93**, 4884 (1990).
26. C.W. Gear, *Numerical Initial Value Problems in Ordinary Differential Equations* (Prentice-Hall, Englewood Cliffs, 1971), p. 154.
27. C.W. Gear, Argonne National Lab Report, ANL-7126, 1966 (unpublished).
28. J. Farges, M.F. de Feraudy, B. Raoult, G. Torchet, J. Chem. Phys. **84**, 3491 (1986).
29. M. Svanberg, N. Marković, J.B.C. Pettersson, Chem. Phys. **220**, 137 (1997).